Chinese Chemical Letters 34 (2023) 107845

Contents lists available at ScienceDirect

Chinese Chemical Letters

journal homepage: www.elsevier.com/locate/cclet

Cysteine-activated fluorescence/photoacoustic integrated probe for non-invasive diagnosis of drug-induced liver injury

Rui Chen, Wenxiu Li, Rong Li, Sixin Ai, Huayong Zhu, Weiying Lin*

Guangxi Key Laboratory of Electrochemical Energy Materials, Institute of Optical Materials and Chemical Biology, School of Chemistry and Chemical Engineering, Guangxi University, Nanning 530004, China

ARTICLE INFO

Article history:
Received 26 May 2022
Revised 15 September 2022
Accepted 21 September 2022
Available online 24 September 2022

Keywords:
Near-infrared fluorescence
Photoacoustic imaging
Fluorescence imaging
Cysteine

ABSTRACT

Hepatotoxicity is a serious problem faced by clinical drugs, and long-term administration or overdose may lead to liver failure and even death of patients. Therefore, developing a reliable detection method for the early diagnosis and therapy of drug-induced liver injury (DILI) has significant meaning. Near-infrared fluorescence (NIRF) and photoacoustic (PA) dual-modality tomography probes can be used for imaging with high sensitivity and high-resolution of disease-related markers in deep tissues. Here, we developed a novel Cys-activated NIRF and PA dual-modality imaging probe (**CDR**) for early diagnosis of DILI, for the first time. The organic molecular probe **CDR** could respond rapidly to Cys, resulting in the absorption peak red-shifted from 560 nm to 725 nm, which also leads to the activation of the PA_{725} signal and $NIRF_{765}$ signal. In addition, the new probe **CDR** could be used for NIRF/PA imaging of exogenous and endogenous Cys level in live cells and mice. More importantly, **CDR** has also been successfully used for *in situ* detection of Cys in early DILI mice and evaluate the therapeutic effect of NAC. Therefore, the **CDR** might become a powerful tool to research the physiological effect of Cys and evaluate the degree of DILI.

As one of the important organs for maintaining life activities, the liver has a variety of functions, such as metabolic synthesis function, detoxification function and immune function [1–3]. Liver damage has become a usual illness in modern medicine, which can progress to hepatocirrhosis or hepatoma, thus causing serious impact on human health and life. Drug-induced liver injury (DILI) is the most common liver injury, which has received extensive attention in modern medicine [4–6]. At present, the existing diagnostic methods of DILI mainly include liver biopsy, histopathological examination, and serum biochemistry [7,8]. However, most of these technologies have disadvantages such as high risk, false positives, and complicated operation steps. Therefore, there is an urgent need to develop a new method for non-invasive, rapid and accurate diagnosis of liver injury.

Cysteine (Cys) is one of the sulfur-containing α-amino acids commonly found in organisms [9]. Within the body, Cys is mainly synthesized from homocysteine through the transmethylation of methionine in the liver, and it participates in the adjustment of redox processes and phospholipid metabolic process [10–12]. In addition, the study found that the increase of Cys concentration in serum was also closely related to the severity of liver injury [13–16]. Therefore, non-invasive *in situ* detecting Cys concentration is completely significant for the diagnosis and treatment of liver injury.

Near-infrared fluorescence (NIR, 650∼900 nm) imaging technology has been widely used to detect the level of Cys *in vivo* due to its advantages of non-invasive and high-sensitivity [17–22]. However, the limited penetration depth of NIR fluorescence probes makes it difficult to image Cys in deep tissues *in vivo* [23–26]. Photoacoustic imaging (PAI) is an emerging non-intrusive biomedical imaging technology with promising outlook, which integrates the superiorities of conventional optics with acoustics imaging, overcome the limitations of conventional optical imaging and achieve high spatial definition imaging of deep tissues in living animals [27–30]. Therefore, near-infrared fluorescence (NIRF) and photoacoustic (PA) dual-mode imaging are expected to achieve the non-invasive and accurate detection of Cys level in deep liver tissues and facilitate the early diagnosis and treatment of DILI. However, there is still a lack of a PA/NIRF bimodal activated probe with deep-penetrating and rapid-response to reveal the role of Cys in drug-induced liver injury. Therefore, based on the advantages of NIRF and PA dual-modality imaging, it is very important to design a fast and robust probe to detect the change of Cys concentration in deep tissues *in vivo*. We hope that this strategy would provide a powerful tool for penetrating deep organization, high spatial resolution and high response rate imaging in liver damage.

* Corresponding author.
E-mail address: weiyinglin2013@163.com (W. Lin).

https://doi.org/10.1016/j.cclet.2022.107845
1001-8417/

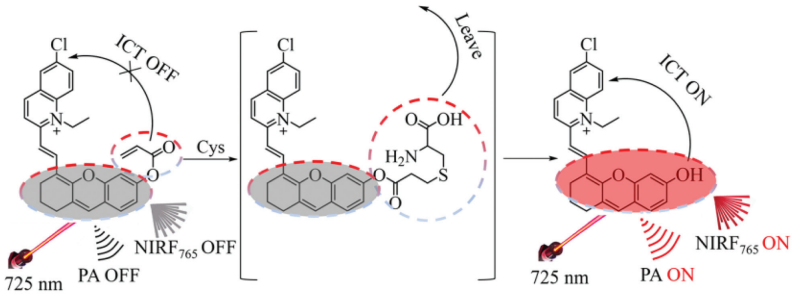

Scheme 1. Rational designs of the NIRF/PA probe **CDR** reporting Cys.

Hence, we rationally designed and synthesized a new NIRF/PA dual-modality small molecule probe **CDR** for noninvasive detection of Cys and diagnosis of liver injury *in vivo*. The dual-modality **CDR** is composed of an acrylate-caged NIR quinolinium-xanthene dye. **CDR** initially has no NIRF and PA signals because it is in a passivation state, weakening the ability of the oxygen atoms to provide electrons. In the presence of Cys, **CDR** can be specifically activated by Cys to turn on its NIRF/PA signals. Due to the complementary advantages of NIRF/PA imaging, the probe **CDR** enable highly sensitive and deep imaging of Cys level at the site of liver injury. Therefore, this NIRF/PA dual-mode probe is expected to provide a new approach for the in-depth study, diagnosis and treatment of liver injury.

The probe **CDR** consists of NIR quinoline-xanthene dye (**CDR-OH**) and an acrylate (Cys response sites). **CDR** itself would be no NIRF$_{765}$/PA$_{725}$ signals due to the intramolecular charge transfer (ICT) effect is suppressed by acrylate groups. When **CDR** reacts with Cys, the acrylate moiety of **CDR** will be hydrolyzed and the hydroxyl group will be released, leading to the recovery of the ICT process and the release of NIRF$_{765}$/PA$_{725}$ signals (Scheme 1). The synthetic route of **CDR** is described in Scheme S1 (Supporting information). Detailed synthesis steps and characterization are given in the Supporting information.

First, the absorption and fluorescence spectra of **CDR** before and after adding Cys were studied. As shown in the Figs. S1A and B (Supporting information), **CDR** had the maximum absorption peak at 560 nm. After the addition of Cys, a new absorption peak appeared at 725 nm, and the color changed from purple to blue. Moreover, **CDR** itself has almost no fluorescence because the acrylate inhibits the ICT process. After the **CDR** reacted with Cys, the NIR fluorescence were observed at 765 nm. These spectral data imply the release of the dye **CDR-OH**. High resolution mass spectrometry (HRMS) data further confirmed the reaction between **CDR** and Cys. The results are shown below. As show in Fig. S2 (Supporting information), a new mass peak appeared at *m/z* 416.1419 after **CDR** reacted with Cys, which is identical to **CDR-OH**. Based on the results of the above data we can speculate that **CDR** could react with Cys to release the dye **CDR-OH** with strong NIR fluorescence signals.

In order to test the recognition effect of Cys by **CDR**, different concentrations of Cys (0~55 μmol/L) were added to **CDR** for reaction, and the absorption and fluorescence emission spectra were recorded. We can get an intuitive data graph. As shown in Fig. 1A, The absorption intensity at 725 nm (Abs$_{725}$) enhanced with the concentration of Cys increase and reached a plateau at about 45 μmol/L Cys concentration. The Abs$_{725}$ intensity has a good linear correlation with Cys concentration in the range of 0~45 μmol/L ($y = 0.00772x + 0.01146$, $R^2 = 0.99344$) and the detection limit was calculated to be 1.25 μmol/L by the equation $3\sigma/k$ (Fig. S3A in Supporting information). In addition, when **CDR** reacted with different concentrations of Cys (0~45 μmol/L), the NIR fluorescence intensity at 765 nm (NIRF$_{765}$) gradually increased (Fig. 1B). The NIRF$_{765}$ intensity has a good linear correlation with Cys concentration in the range of 0~45 μmol/L ($y = 9.20227x + 58.93716$, $R^2 = 0.9988$), and the detection limit was calculated to be 0.7584 μmol/L by the equation $3\sigma/k$ (Fig. S3B in Supporting information). These results indicate that **CDR** has an excellent response to Cys *in vitro*. The photoacoustic signal of **CDR** was measured under different excitation wavelengths. As shown in (Fig. 1C), the pure probe showed no obvious signal changes, while the probe showed the maximum photoacoustic signal intensity at 725 nm under the action of cysteine. Next, we further investigated the PA responses of **CDR** to different concentrations of Cys. As the concentration of Cys increased, the strength of PA$_{725}$ gradually increased, and the color of the reaction liquid changed from purple to blue (Fig. 1D). The PA$_{725}$ intensity has a good linear correlation with concentration of Cys (0~45 μmol/L) ($y = 20.54714x + 21.6999$, $R^2 = 0.9983$), the detection limit was calculated as 2.07 μmol/L by the $3\sigma/k$ equation (Fig. S3C in Supporting information). We next investigated the response time of **CDR** to Cys *in vitro*. As show in Fig. 1E and Fig. S4 (Supporting information), the Abs$_{725}$ and NIRF$_{765}$ signal enhanced with the increase of the reaction time between the probe **CDR** and Cys, and reached a plateau within 5 min, indicating **CDR** can detect Cys rapidly. To evaluate the selectivity of **CDR**, we investigated the probe recognition of other biologically relevant analytes, such as biothiols, reactive oxygen species (ROS) (Fig. 1F), no absorption response was observed, indicating that **CDR** has high selectivity for Cys. These results demonstrate that **CDR** had a good photoacoustic/fluorescent response to Cys, which is expected to provide a method for detecting of Cys in deep tissues *in vivo*.

In addition, the response of the probes to Cys was also evaluated under different pH conditions. The Abs$_{725}$ and NIRF$_{765}$ signals of **CDR** remained almost unchanged at pH 3.0~6.0. After adding Cys, **CDR** exhibited a good signal enhancement of Abs$_{725}$ and NIRF$_{775}$ in the pH range of 6.0~7.5, indicating that **CDR** could detect Cys under a wide range of pH physiological conditions (Figs. S5A and B in Supporting information). These results indicate that **CDR** has a fast NIRF/PA dual signal response to Cys *in vitro*, it has the potential of detecting cysteine sensitively in living cells and deep tissues *in vitro*.

With the results of optical experiment, we further studied **CDR** imaging of Cys in living cells by NIRF/PA imaging technique. The biocompatibility of the probe was fist studied before cell imaging [31]. Human normal hepatocytes cells (HL-7702) and human hepatoma cells (HepG2) were cultured with different concentrations of **CDR** (0–50 μmol/L) for 24 h, and then the cell activity was detected by methyl thiazolyl tetrazolium (MTT) assay. When the 50 μmol/L **CDR** was incubated with cells, the HL-7702 and HepG2 cells viability was still higher than 80%, this indicated that **CDR** has low toxicity to cells and can be used to image Cys *in vivo* (Fig. S6 in Supporting information). It is well known that Acetaminophen (APAP) is a commonly used medicine for reducing fever, pain and colds. However, long-term or excessive use of APAP

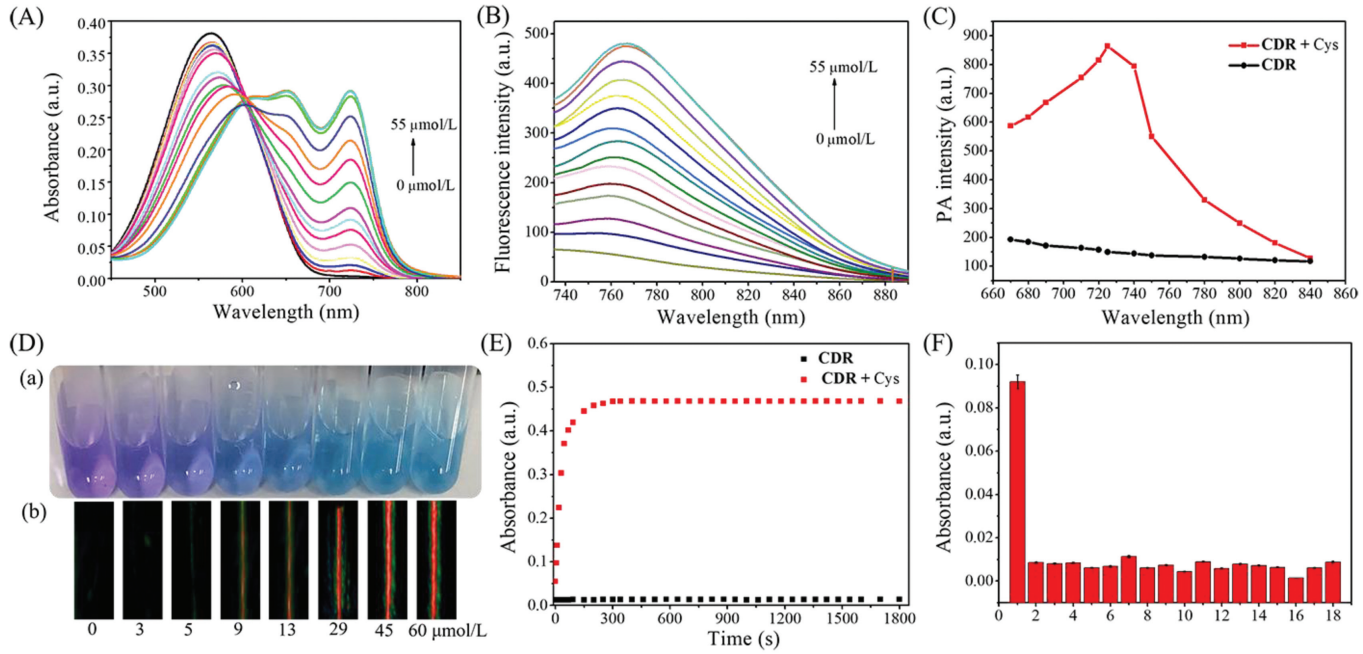

Fig. 1. Spectroscopic experiments of **CDR**. (A) Absorption spectra of **CDR** (10 μmol/L) with varied concentrations of Cys (0~55 μmol/L). All spectra were tested after 20 min at 25 °C in PBS buffer (pH 7.4, 25% DMSO, v/v). (B) Fluorescent spectrum of **CDR** (10 μmol/L) with varied concentrations of Cys (0~55 μmol/L). (C) PA intensity of **CDR** with and without Cys (45 μmol/L) for different wavelength excitations. (D) The color image after the reacting of each solution. (E) Time-dependent Abs_{725} changes with the addition of Cys (45 μmol/L). (F) Absorbance of **CDR** (10 μmol/L) at 725 nm for various analytes. 1, Cys; 2, Pro; 3, Ser; 4, Phe; 5, Ala; 6, Met; 7, GSH; 8, Arg; 9, Tyr; 10, Asp; 11, His; 12, KCl; 13, $ZnCl_2$; 14, H_2O_2; 15, NaOH; 16, NaClO; 17, Na_2SO_4; 18, $FeSO_4$. Concentration: Cys, GSH, Hcy, H_2O_2, 150 μmol/L; other analytes, 300 μmol/L.

could lead to liver damage and even death [32,33]. To validate the potential of probe for NIRF/PA imaging *in vivo*, NIRF/PA imaging of cells was first performed. After incubation with **CDR** for 30 min, HL-7702 cells showed no obvious NIRF and PA signals. However, when cells were pretreated with APAP (50 μL, 1 mmol/L) for 1 h and cultured with the **CDR** for 30 min, high NIRF and PA signals were observed. When cells were stimulated with APAP and then treated with 3 mmol/L NAC for 2 h, (NAC is *N*-acetyl-L-cysteine, a therapeutic agent for liver injury) [34–36], the PA and NIRF signals were significantly reduced (Figs. S7A-C in Supporting information). These results confirmed that the turn-on of the NIRF/PA response should be attributed to the presence of endogenous Cys in HL-7702 cells, and NAC can be used to treat cell injury resulted in significantly enhanced of NIRF/PA. These results indicate that **CDR** has good biocompatibility and could be used for NIRF/PA dual-modality imaging of Cys in living cells.

Before performing *in vivo* PA imaging, the probe *in vivo* toxicity was first investigated. All animal experiments were performed in compliance with the relevant laws and approved by the Animal Care and Experiment Committee of Guangxi University (protocol number: Gxu-2021–115). Compared with the control group, mice treated with **CDR** showed no casualties and a slight increase in body weight, indicating that **CDR** has good biocompatibility (Fig. S8 in Supporting information). **CDR** and Cys were injected into the high region of interest (ROI) L of mouse legs to test the ability of **CDR** to recognize Cys *in vivo*. When injected with **CDR** (100 μL, 30 μmol/L) for 30 min, ROI L showed obvious PA_{725} signals (Fig. 2A). However, when the ROI R region was pretreated with 1 mmol/L *N*-ethylmaleimide (NEM, a cysteine inhibitor) for 3 h, followed by subcutaneous injection of probes for 30 min, the PA signal was significantly attenuated compared with the only **CDR** injected group. These results indicate that the probe could achieve PA imaging of Cys in live mice. However, after injection of exogenous Cys (50 μL, 1 mmol/L), the ROI R region exhibited stronger PA signal than the pure **CDR** group (Figs. 2A and B). The results suggest that **CDR** is suitable for PA imaging of endogenous and exogenous Cys *in vivo*.

Next, the ability of **CDR** for real-time monitoring of endogenous Cys and non-invasive *in-situ* visualization of early DILI diagnosis was evaluated. First, three groups of healthy mice were injected with different doses of APAP (0, 150, 300 mg/kg) through the tail vein. As shown in (Fig. 2C), there were slight change in fluorescence signal in the liver of healthy mice after injected of **CDR** (control group). This indicates that **CDR** could be enriched in the liver and identify of endogenous Cys *in vivo*. Initially, no fluorescence signal was given to the liver region of mice with a small dose of APAP (150 mg/kg), but as the drug was administered over time, the fluorescent signal in the liver region gradually enhanced, and reached a maximum intensity of 4 h. We found that when mice were injected with high dose of APAP (300 mg/kg) for 4 h, the PA signal intensity of liver became observably higher than the pure **CDR** group, suggesting that the concentration of Cys in the liver increased with the aggravation of DILI. These experiments demonstrate that **CDR** can image Cys level during the development of APAP-induced acute liver injury (Figs. 2C and D). It is worth noting that the fluorescence signal gradually decreased after 4 h, which we speculated was because **CDR** was excreted from the body by metabolism. These experiments demonstrate that **CDR** could enable real-time *in situ* identification of Cys level during the development of APAP-induced early liver injury.

To further demonstrate that the probe can image Cys level in the liver, six important organs of the control group and the APAP-induced liver injury model group (2 h, 4 h and 7 h) were dissected for *in vitro* fluorescence imaging. The spleen, kidney, lung, liver, stomach, and heart were subjected to fluorescence imaging at 720 nm excitation as shown in Fig. S9 (Supporting information). The experimental results showed that only the liver had fluorescent signal, and the fluorescent signal of APAP group were stronger than those of control group, which further indicated that APAP-induced early liver injury would lead to the increase of Cys level.

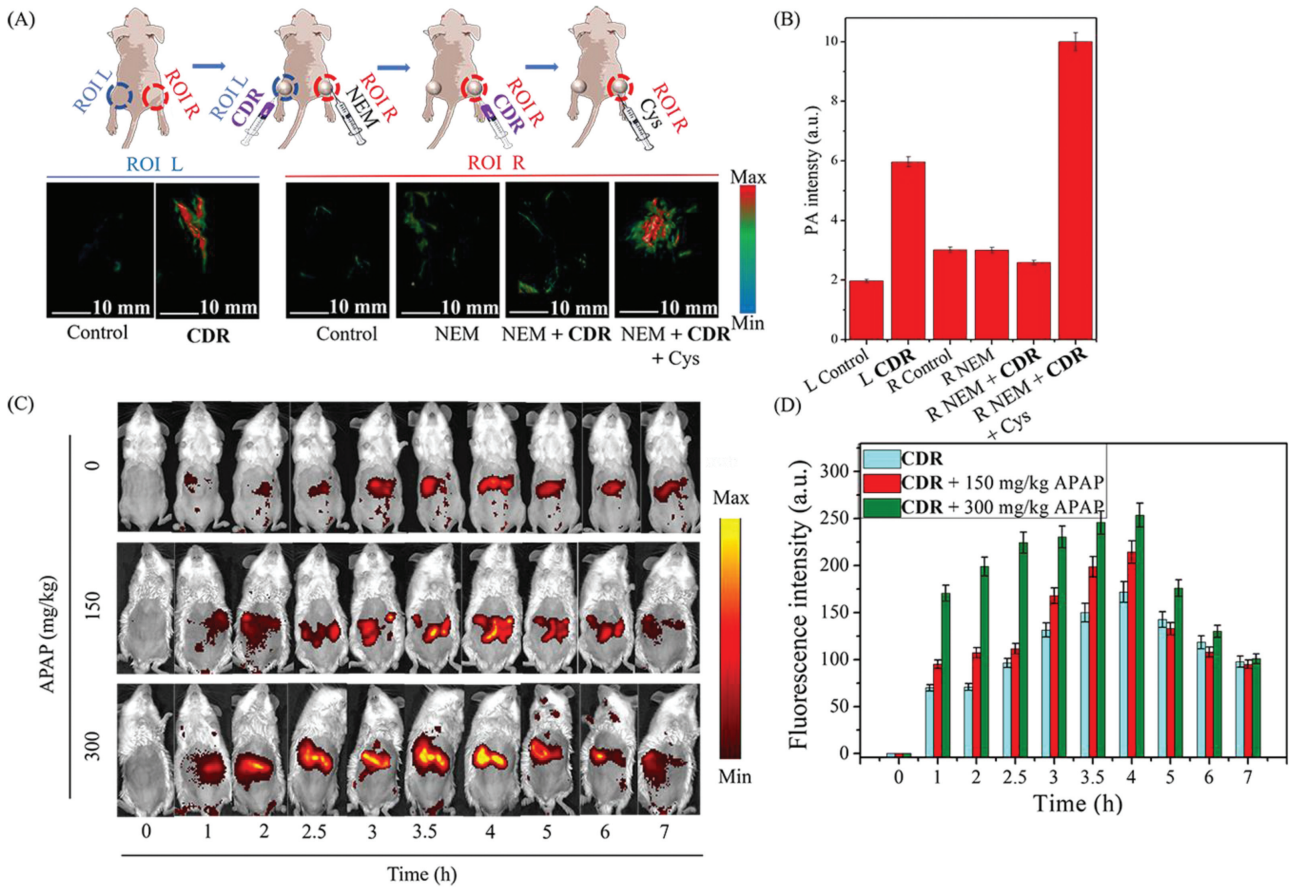

Fig. 2. Endogenous and exogenous fluorescence imaging and PA imaging in living mice. (A) Exogenous PA imaging of mouse leg. (ROI) L was injected with **CDR** (100 μL, 30 μmol/L) for 30 min, (ROI) R was injected with NEM (100 μL, 1 mmol/L) for 3 h and then injected with **CDR** (100 μL, 30 μmol/L) for 30 min after imaged inject of exogenous Cys (50 μL, 1 mmol/L). (B) Image of experimental data of exogenous PA in mice. (C) Fluorescence imaging of mice with different degrees of liver injury. Three rats were injected **CDR** (100 μL, 30 μmol/L) through the tail vein and then injected separately with APAP (0, 150 and 300 mg/kg) through the tail vein to establish liver injury, and collect real-time fluorescence signal images under the excitation of 720 nm laser. (D) $NIRF_{765}$ signal intensity values from (C).

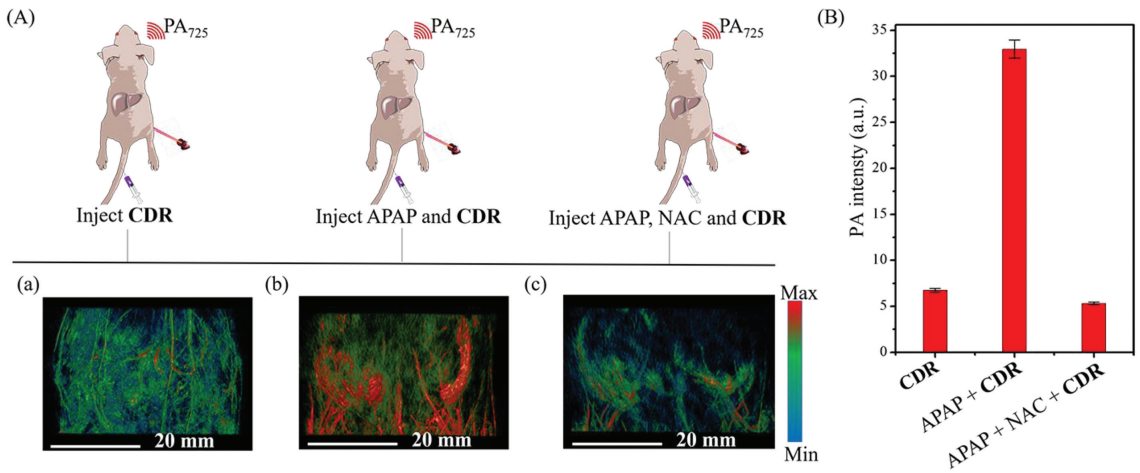

Fig. 3. (A) *In vivo* PA imaging of mouse liver injury model. (a) There was no obvious PA signal in liver when injected **CDR** (100 μL, 30 μmol/L) into caudal vein for 3 h. (b) A liver injury model was established by APAP (300 mg/kg) for 4 h and then **CDR** (100 μL, 30 μmol/L) was injected into caudal vein for 3 h. PA imaging showed strong fluorescence. (c) After a caudal vein injection of APAP for 4 h to establish a liver injury model, the PA imaging signal was significantly weakened after caudal vein injection of NAC (100 μL, 3 mmol/L) for 4 h and tail vein injection of **CDR** for 3 h. (B) The Photoacoustic signal intensity in mice.

Therefore, this probe **CDR** can be used to diagnose APAP-induced early liver injury process.

The ability of **CDR** to monitor endogenous Cys and non-invasively diagnose DILI was assessed. The experimental results are shown in Fig. 3A, there were no obvious PA signal in liver when injected of **CDR** (100 μL, 30 μmol/L) for 3 h. After pretreatment with 300 mg/kg APAP for 4 h and injected with **CDR** (100 μL, 30 μmol/L) for 3 h, the liver PA signal intensity was greatly increased compared with the control group. Notably, when the hepatoprotective agent NAC (100 μL, 3 mmol/L) was injected into DILI mice for 4 h, a significant attenuation of the PA signal at the liver site was observed, which was consistent with the NIRF/PA

imaging results of NAC-treated cells (Fig. 3B). This indicates that the probe could be used for pathological diagnosis and therapeutic evaluation of early liver injury mice by non-invasive PA imaging technology.

In conclusion, we constructed a novel probe **CDR** for diagnosing drug-induced early liver injury *in vivo* by NIRF and PA dual-mode imaging, for the first time. **CDR** exhibited obvious NIRF/PA dual-signal responses to Cys with high sensitivity with fast response speed and high sensitivity. In addition, the probe **CDR** has been successfully performed NIRF/PA imaging of intracellular Cys level. More importantly, in the APAP-induced early-stage liver injury model in mice, **CDR** could not only diagnosed liver injury by *in situ* monitoring of hepatic Cys level, but also evaluated the repair effect of NAC drugs on liver injury. Based on the excellent performance of the NIRF/PA dual-modality **CDR**, we hope this work would provide new ideas for the early diagnosis and pathogenesis of DILI.

Declaration of competing interest

The authors declare that they have no known competing financial interests or personal relationships that could have appeared to influence the work reported in this paper.

Acknowledgments

This work was funded by the National Natural Science Foundation of China (Nos. 21672083, 21877048, 22077048), Natural Science Foundation of Guangxi (Nos. 2021GXNSFDA075003, AD21220061), and the Startup Fund of Guangxi University (No. A3040051003).

Supplementary materials

Supplementary material associated with this article can be found, in the online version, at doi:10.1016/j.cclet.2022.107845.

References

[1] K. Ray, Nat. Rev. Gastro. Hepat. 15 (2018) 130–131.
[2] T. Akaike, T. Ida, F.Y. Wei, et al., Nat. Commun. 8 (2017) 1177.
[3] M. Fellner, E. Siakkou, A.-S. Faponle, et al., J. Biol. Inorg. Chem. 21 (2016) 501–510.
[4] Y. Zhou, J. Wang, D. Zhang, et al., Chin. Med. UK 16 (2021) 135.
[5] R.J. Andrade, N. Chalasani, E.S. Björnsson, et al., Nat. Rev. Dis. Primers. 5 (2019) 58.
[6] J.S. Au, V.J. Navarro, S. Rossi, Aliment. Pharm. Ther. 34 (2011) 11–20.
[7] R.A. Nathwani, S. Pais, T.B. Reynolds, N. Kaplowitz, Hepatology 41 (2005) 380–382.
[8] J. Ozer, M. Ratner, M. Shaw, W. Bailey, S. Schomaker, Toxicology 245 (2008) 194–205.
[9] X. Chen, Y. Zhou, X. Peng, J. Yoon, Chem. Soc. Rev. 39 (2010) 2120–2135.
[10] G.B. Steventon, S. Khan, S.C. Mitchell, J. Pharm. Pharmacol. 70 (2018) 1069–1077.
[11] T. Rehman, M.A. Shabbir, M. Inam-Ur-Raheem, et al., Food. Sci. Nutr. 8 (2020) 4696–4707.
[12] C.M. Hunt, J.I. Papay, V. Stanulovic, A. Regev, Hepatology 66 (2017) 646–654.
[13] S.A. Seifert, D. Kovnat, V.E. Anderson, et al., Toxicol. Lett. 54 (2016) 282–285.
[14] A. Pastore, A. Alisi, G. Di Giovamberardino, et al., Int. J. Mol. Sci. 15 (2014) 21202–21214.
[15] L. Yue, H. Huang, W. Song, W. Lin, Chem. Eng. J. 441 (2022) 135981.
[16] W. Li, R. Li, R. Chen, et al., Anal. Chem. 93 (2021) 8978–8985.
[17] J. Xu, J. Pan, Y. Zhang, et al., Sens. Actuators B 238 (2017) 58–65.
[18] R. Zhang, J. Yong, J. Yuan, Z. Xu, Coordin. Chem. Rev. 408 (2020) 213182.
[19] L. Yuan, W. Lin, K. Zheng, L. He, W. Huang, Chem. Soc. Rev. 42 (2013) 622–661.
[20] S. Cai, C. Liu, X. Jiao, L. Zhao, X. Zeng, J. Mater. Chem. B 8 (2020) 2269–2274.
[21] H. Ren, F. Huo, Y. Zhang, S. Zhao, C. Yin, Sens. Actuators B 319 (2020) 128248.
[22] Y. Yang, T. Zhou, M. Jin, et al., J. Am. Chem. Soc. 142 (2020) 1614–1620.
[23] A. Tarai, Y. Li, B. Liu, et al., Coordin. Chem. Rev. 445 (2021) 214070.
[24] X. Wu, W. Shi, X. Li, H. Ma, Acc. Chem. Res. 52 (2019) 1892–1904.
[25] X. Li, X. Liang, J. Yin, W. Lin, Chem. Soc. Rev. 50 (2021) 102–119.
[26] T. Li, F. Huo, J. Chao, C. Yin, Chem. Commun. 56 (2020) 11453–11456.
[27] R. Li, W. Li, R. Chen, W. Lin, Sens. Actuators B 347 (2021) 130616.
[28] X.P. Fan, W. Yang, T.B. Ren, et al., Anal. Chem. 94 (2022) 1474–1481.
[29] C. Zhang, Z. Qiu, L. Zhang, et al., Chem. Sci. 12 (2021) 4883–4888.
[30] W. Li, R. Li, R. Chen, et al., Anal. Chem. 94 (2022) 7996–8004.
[31] H. Yan, F. Huo, Y. Yue, J. Chao, C. Yin, J. Am. Chem. Soc. 143 (2021) 318–325.
[32] D. Chen, H.-M. Ni, L. Wang, et al., Hepatology 69 (2019) 2164–2179.
[33] X. Shi, H. Bai, M. Zhao, et al., Transl. Res. 196 (2018) 31–41.
[34] Y. Ntamo, K. Ziqubu, N. Chellan, et al., Oxid. Med. Cell. Longev. 2021 (2021) 3320325.
[35] G.P. Sreekanth, J. Panaampon, A. Suttitheptumrong, et al., Antiviral. Res. 166 (2019) 42–55.
[36] H. Jaeschke, J.Y. Akakpo, D.S. Umbaugh, A. Ramachandran, Toxicol. Sci. 174 (2020) 159–167.